Photodynamic Therapy Agent with a Built-In Apoptosis Sensor for Evaluating Its Own Therapeutic Outcome in Situ

Klara Stefflova,[†] Juan Chen,[‡] Diane Marotta,[‡] Hui Li,[‡] and Gang Zheng*[,‡]

Departments of Chemistry and Radiology, University of Pennsylvania, Philadelphia, Pennsylvania 19104

Received February 8, 2006

Identifying the extent of apoptosis in cells or tissues after cancer therapy in real time would be a powerful firsthand tool for assessing therapeutic outcome. We combined therapeutic and imaging functions in one agent, choosing photodynamic therapy (PDT) as an appropriate cancer treatment modality. This agent induces photodamage in irradiated cells and simultaneously identifies apoptotic cells by near-infrared fluorescence. This photodynamic therapy agent with a built-in apoptosis sensor (PDT-BIAS) contains a fluorescent photosensitizer used as an anticancer drug, connected to a fluorescence quencher by a caspase-3 cleavable peptide linker. We demonstrated that cleavage of the peptide linker by caspase-3, one of the executioner caspases involved in apoptosis, results in a detectable increase of fluorescence in solution and in cancer cells after PDT treatment. The apoptosis involvement and drug effectiveness were confirmed by Apoptag and cell viability (MTT) assays supporting the ability of PDT-BIAS to induce and image apoptosis in situ.

Introduction

Apoptosis is essential for the normal development of a multicellular organism but its disregulation leads to severe diseases[1] including cancer.[2] Many anticancer drugs act against this malfunction, killing the cells by restoring their programmed cell death. Apoptosis is characterized by the ordered manner in which the damaged or otherwise compromised cells die. This form of active death is very different from necrosis which results in an uncontrolled bursting of cells followed by an inflammatory reaction.[3] Common methods of imaging apoptosis[4,5] focus mainly on the early stages where the differences between apoptosis and necrosis are most pronounced.[6] They use features of controlled cell degradation such as disruption of mitochondrial transmembrane potential, activation of caspases, DNA laddering (e.g. TUNEL/Apoptag assay), redistribution of phospholipids in the plasma membrane (e.g. Annexin V-FITC membrane binding) and formation of apoptotic bodies.[7,8] Independent of the stimuli, most apoptotic pathways reach the activation of caspase-3, an executioner caspase usually indicating the point of no-return.[9] This protease, being a specific indicator of apoptosis, is an attractive, useful, and unambiguous target for apoptosis imaging.

Photodynamic therapy (PDT) is a promising cancer treatment modality[10,11] that involves a photosensitizer (PS), light, and molecular oxygen. The tumor-associated photosensitizer,[12] after activation with light of an appropriate wavelength, produces reactive oxygen species, mainly singlet oxygen.[13] This cytotoxic effector of PDT acts locally due to its short lifetime resulting in an average 20 nm diffusion range from the site of generation.[11,14] Therefore, the localization of PS in the cell is also the scene of organelle damage.[15] The desired outcome of PDT is cell death.[16] The type of cell death caused by PDT (apoptosis vs necrosis) depends on a number of factors[17,18] including the type and size of tumor, PDT treatment conditions, as well as the type of photosensitizer[19] and its site of accumulation.[20] It has been shown that when the photosensitizer targets mitochondria or endoplasmic reticulum (but not plasma membrane) it is primarily the apoptotic response that leads to cell death.[21,22] To noninvasively image PDT-induced early apoptosis in situ would, together with the well-established in vitro and ex vivo assays, help to assess the best PDT conditions for each photosensitizer and tumor type and ultimately enable adjustment of the protocol for each patient (patient-tailored treatment). The in situ imaging is possible since the photosensitizer's fluorescence in the near-infrared (NIR) region[23] corresponds to the therapeutic wavelength range with deep tissue penetration.

We have designed a probe that is both a therapeutic and imaging agent in the sense that it combines its original role in treating cancer with the ability to directly assess its own therapeutic outcome by monitoring PDT-induced apoptosis. It contains a photosensitizer that acts as both a drug and a fluorescent label, and a fluorescence quencher bound to the opposing sites of a caspase-3 cleavable peptide linker which holds the photosensitizer and quencher in close proximity enabling FRET.[a] After this construct enters a cell and is activated by light, the photosensitizer produces singlet oxygen that damages the cell. If the damage is sufficient but not catastrophic, the apoptotic cascade starts and caspase-3 is processed to its active form indicating initiation of irreversible apoptotic death.[9,24] Once activated, this protease cleaves the peptide linker, thus separating the photosensitizer from the fluorescence quencher and restoring its fluorescence (Scheme 1). Therefore, the cells actually dying by apoptosis can be visualized by NIR fluorescence. In this way, PDT-BIAS is capable of visualizing its own therapeutic outcome.

We designed a prototype PDT-BIAS using pyropheophorbide *a* (Pyro), a photosensitizer which localizes near mitochondria[25−27] and induces apoptosis upon irradiation.[26,28] This semisynthetic PS, obtained by three steps from *Spirulina* algae, has a long-wavelength absorption (665 nm) and emission (675 and 720

* To whom correspondence should be addressed. Phone: 1-215-898-3105. Fax: 1-215-746-8764. E-mail: Gang.Zheng@uphs.upenn.edu.
[†] Department of Chemistry.
[‡] Department of Radiology.

[a] Abbreviations: DCM, dichloromethane; ESI-MS, electrospray ionization mass spectrometry; FRET, fluorescence resonance energy treansfer; HPLC, high performance liquid chromatography; MALDI-ToF, matrix assisted laser desorption/ionization−time-of-flight mass spectrometry; MTT, 3-[4,5-dimethylthiazol-2-yl]-2,5-diphenyl tetrazolium bromide; NMP, 1-methyl-2-pyrrolidinone; RT, retention time; TFA, trifluoroacetic acid; TIS, triisopropylsilane; UV−vis, ultraviolet−visible spectroscopy.

10.1021/jm060146u CCC: $33.50
Published on Web 05/28/2006

Scheme 1. Schematic of PDT-BIAS Function[a]

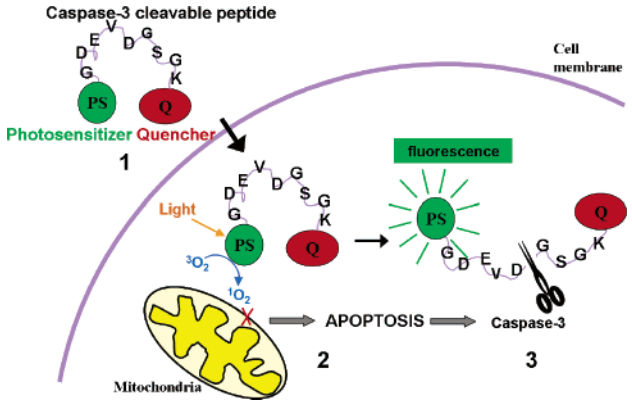

[a] (1) PDT-BIAS accumulates in tumor cells; fluorescence is quenched in the native state. (2) Singlet oxygen is produced upon light activation and apoptosis is triggered. (3) Activated caspase-3 cleaves the peptide and fluorescence is restored, indicating the apoptotic cells.

nm), good singlet oxygen yield (over 50%), no dark toxicity,[27] and its derivative Photochlor is in phase I/II clinical trial.[29] BHQ-3 (black hole quencher 3, absorption max at 672 nm) was chosen as an appropriate quencher of Pyro's fluorescence via FRET and G*DEVD*GSGK was used as a previously described caspase-3 cleavable peptide linker[30,31] with the cleavage site between D and G and recognition site in italics.

Results and Discussion

To validate this concept we needed to determine whether our prototype compound (1) is specifically cleaved by caspase-3, (2) is able to enter cells, (3) causes cell death, (4) is cleavable as a consequence of apoptosis, and (5) can image apoptosis using its restored fluorescence. The substrate specificity was confirmed by HPLC and fluorescence restoration measured after the cleavage with caspase-3 in solution. To prove that our quenched PDT-BIAS, Pyro-GDEVDGSGK-(BHQ-3) (PPB), can enter cells, several fluorescent control molecules substituting the BHQ-3 quencher were synthesized and visualized by laser scanning confocal microscopy in the cancer cell cytoplasm. Cell viability (MTT) assay, in which living cells reduce the colorless MTT to the purple formazan product measurable by UV−vis spectroscopy, was used for assessing the PDT efficacy for different light and drug doses. Using confocal microscopy, we detected an increase of fluorescence inside of the cells incubated with PPB and treated by light. As expected, the increase of fluorescence was a result of *apoptosis*-induced cleavage of the peptide linker as confirmed by the Apoptag method and anticaspase-3 staining. Therefore, by detecting apoptosis in cancer cells using our prototype PDT-BIAS and other well-established methods, we have demonstrated that the photodamage induced by PDT-BIAS causes apoptosis and can be consequently visualized using the same molecule by tracking the NIR fluorescence signal.

Synthesis of PPB. The synthesis started by solid-phase peptide synthesis (SPPS), giving Fmoc-GDEVDGSGK on Sieber resin (**1**). The photosensitizer Pyro acid was then coupled to the N-terminus of the immobilized peptide (Figure 1), giving Pyro-GDEVDGSGK-Sieber resin (**2**) that was cleaved from the solid phase and deprotected with 50% TFA. The BHQ-3-NHS quencher was coupled in a solution reaction to the C-terminal lysine of Pyro-GDEVDGSGK (PP, **3**), and the product Pyro-GDEVDGSGK-(BHQ-3) (PPB, **4**) (and a small sample of compound **3**) was purified by HPLC and characterized by UV−vis and MALDI-ToF (Supporting Information, Figures 1 and 2).

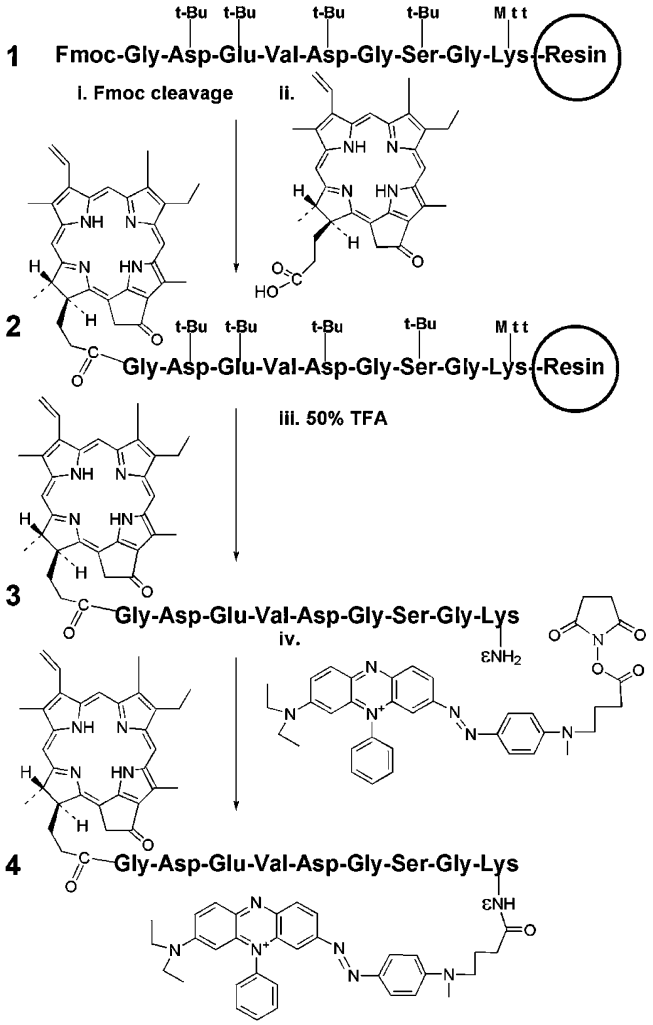

Figure 1. Pyro-GDEVDGSGK-(BHQ-3) (PPB, **4**) synthesis.

Cleavage by Caspase-3 in Solution. We needed to confirm that (1) PPB is cleavable by caspase-3, (2) the fluorescence of Pyro is effectively quenched by BHQ-3 when restrained by the peptide linker, and (3) this fluorescence is restored after cleavage. We demonstrated this using two solution assays—HPLC for monitoring the cleavage of PPB by purified caspase-3 in solution and fluorescence spectroscopy for detecting the consequent fluorescence restoration. The HPLC chromatogram shows that PPB (RT 26.693 min) is stable in the cleavage buffer (Figure 2A), but two fragments (RT 12.787 and 25.087 min) were generated from an intact molecule (RT 26.709 min) when incubated with caspase-3 for 50 min (Figure 2B). The cleavage is prevented (RT 26.708 min) when caspase-3 specific inhibitor (Ac-DEVD-CHO) is added to the solution of PPB and caspase-3 (Figure 2C). An immediate increase of fluorescence which plateaus at 90 min was monitored by fluorescence spectroscopy (Figure 2D) for PPB incubated with caspase-3 (■). This increase was not observed for PPB alone in buffer (●) or PPB incubated with caspase-3 and caspase-3-specific inhibitor (▲) or for a scrambled sequence **s**PPB (□, Pyro-GPLGLARK-(BHQ-3)) incubated with caspase-3 (HPLC in Supporting Information, Figure 3), indicating that this cleavage is caspase-3 specific. These assays demonstrate that PPB can be specifically cleaved by caspase-3 in solution, and as a result, there is an 8-fold increase of fluorescence.

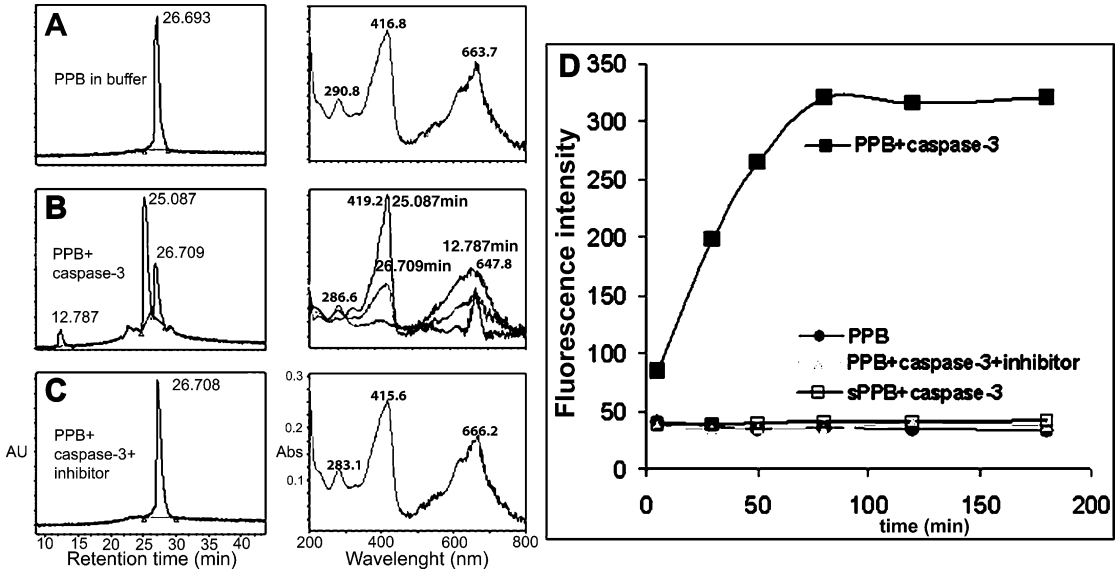

Figure 2. Cleavage of Pyro-GDEVDGSGK-(BHQ-3) (PPB, **4**) by caspase-3 in solution results in the formation of two fragments and a fluorescence increase that was monitored by HPLC and fluorescence spectroscopy assays. HPLC assay (A−C): HPLC chromatogram at 410 nm (left column), UV−vis spectra of corresponding peak (right column). Single peak of PPB alone incubated in the buffer for 50 min (A), supports its chemical stability. Incubation of PPB (RT 26.709 min) with caspase-3 for 50 min (B) results in formation of two fragments with RT 12.787 min and 25.087 min. This is prevented when PPB is incubated with caspase-3 and caspase-3 inhibitor for 50 min (C). Fluorescence assay (D): Fluorescence intensity increases when PPB is incubated with caspase-3 (■) compared to the stable background fluorescence of PPB alone (●), PPB incubated with caspase-3 and caspase-3 inhibitor (▲), and sPPB (□) (scrambled sequence Pyro-GPLGLARK-(BHQ-3)) incubated with caspase-3, all monitored for 3 h, confirming PPB's stability and caspase-3 specificity.

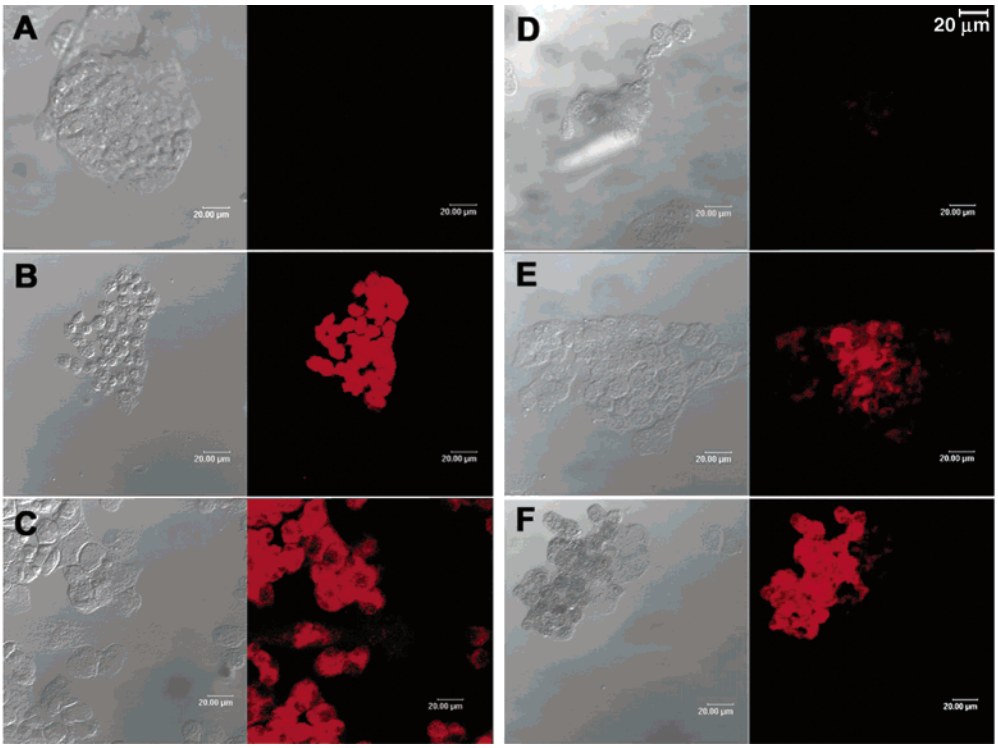

Figure 3. Accumulation and cleavage of Pyro-GDEVDGSGK-(BHQ-3) (PPB) inside the hepatoblastoma G_2 cells. Confocal images of (A) $HepG_2$ cells alone, (B) $HepG_2$ cells incubated for 24 h with Pyro-GDEVDGSGK (PP, **3**, 200 μM), and (C) $HepG_2$ cells incubated for 24 h with Pyro-GDEVDGSGK-Fluorescein (PPFl, 200 μM), showing that both PP and PPFl (used as PPB analogues) accumulate in the cytoplasm; (D) $HepG_2$ cells incubated for 24 h with PPB (200 μM) show minimal fluorescence increase, excluding apoptosis-independent PPB decomposition; (E) $HepG_2$ cells incubated for 30 min with PPB (200 μM) and treated with 5 J/cm^2 light dose and (F) $HepG_2$ cells incubated for 24 h with PPB (200 μM) and treated with 5 J/cm^2 light dose, both showing significant increase of fluorescence from PDT-triggered apoptosis-induced PPB cleavage. In each case, the left image is DIC and the right image is Pyro fluorescence (scale bar (upper right corner) represents 20 μm).

Accumulation and Cleavage of PPB in Cancer Cells. Given PPB's large size, it is important to determine if it can enter cells. We synthesized two model fluorescent molecules whose size and properties are similar to those of PPB: Pyro-GDEVDGSGK (PP, **3**, no quencher) and Pyro-GDEVDGSGK-Fluorescein (PPFl). Unlike the quenched PPB, these analogues can be visualized by confocal microscopy. A strong fluorescence signal is localized in the cytoplasm of the cells incubated for 24 h with PP (Figure 3B) and PPFl (Figure 3C) when compared with untreated cells (Figure 3A). Taking advantage of PPB's

weak intrinsic fluorescence, we were able to visualize even the intact molecule inside living cells using a more sensitive fluorescence microscope (Supporting Information, Figure 4). This confirmed that Pyro can serve as a nonspecific cell delivery vehicle even for molecules with a mass around 2000 Da.

The ability of PPB to be cleaved as a consequence of PDT-induced apoptosis was also monitored using confocal microscopy. Hepatoblastoma G_2 cells ($HepG_2$) were incubated with PPB (200 μM) for either 30 min or 24 h and subsequently treated with a 5 J/cm^2 light dose using a 670 nm laser (parts E and F of Figure 3, respectively). The PDT-treated cells (Figure 3E,F) show a significant increase of fluorescence intensity. In contrast, the control cells (Figure 3D) incubated with PPB for 24 h without exposure to light showed a minimal fluorescence increase. We have also performed a control experiment showing that the increase of fluorescence for PDT-treated cells previously incubated with Pyro-GDEVDGSGK-(BHQ-3) (**4**) is greater than for those PDT-treated cells incubated with scrambled sequence Pyro-GHSSK(BHQ-3)LQL (Supporting Information, Figure 5). These results confirmed that the peptide linker in the PDT-BIAS can be cleaved inside the PDT-treated cells and that the significant increase of Pyro's fluorescence is induced by apoptosis-specific cleavage. This increase is not simply due to PPB decomposition over a period of 24 h (Figure 3D) or nonspecific proteolytic degradation (Supporting Information, Figure 5). This cleavage was also monitored by Flow cytometry in KB cells (human epidermoid carcinoma cells) incubated with 15μM PPB, showing that the cells treated with light (10 J/cm^2 light dose) display 1.7−2.4-fold fluorescence increase compared to those kept in the dark.

Confirmation of Apoptosis Involvement. To ensure that PDT-BIAS is indeed reporting apoptosis, an independent evaluation of apoptosis is required. One of the hallmarks of apoptosis is DNA laddering. This specific DNA cleavage indicates a point of no return in cell death that critically depends on caspase-3 activity and can be detected by an Apoptag (TUNEL) assay. We used this well-established method to visualize apoptotic cells by monitoring Fluorescein fluorescence from the Apoptag assay using confocal microscopy. The $HepG_2$ cells that were incubated with PPB, treated with PDT, and then stained with Apoptag (Figure 4D) show a clear increase of fluorescence in both the Fluorescein (488 nm) and Pyro (633 nm) fluorescence channels compared to cells alone (Figure 4A) and cells incubated with both PPB and Apoptag but not treated with PDT (Figure 4B). The coexistence of fluorescence from both Pyro (as a result of the caspase-3-dependent cleavage of PDT-BIAS) and Fluorescein (arising from labeling of the apoptosis-induced DNA cleavage in the Apoptag assay) in the PDT- and Apoptag-treated cells (Figure 4D) demonstrates that PDT-BIAS can induce and image apoptosis in vitro. The simultaneous appearance of both signals is not due to the Pyro fluorescence leaking into the Fluorescein channel, as shown in Figure 4C.

Also, staining the cells with fluorescently labeled antibody against activated caspase-3 supported this Apoptag data. Using flow cytometry, the KB cells incubated with 15 μM PPB and treated with PDT showed a significant (1.5−2.9-fold) increase in anticaspase-3 staining compared to those incubated with drug but kept in dark.

PDT-Induced Cell Death. Apoptosis induction correlates with PDT-BIAS cleavage in single cells (Figure 4), but for quantitation of overall cell death in the whole population for variable drug and light doses, we used an MTT assay. This is a standard method of determining the PDT efficacy of a drug by correlating the viability of cells before and after PDT treatment, where cells not treated with light and drug serve as a relative reference (100% viable). We have confirmed (as shown in Figure 5) that (1) Pyro has a minimal dark toxicity since the viability of cells incubated with even the highest PPB dose (30 μM) but not treated with light (white column, 0 J/cm^2) is similar to that of the control cells, (2) increased drug or light doses led to decreased cell viability (ANOVA test included in Supporting Information), and (3) cells treated with 7.5 J/cm^2 (the highest light dose) have reduced viability below 10% of that of control cells when incubated with even the lowest PPB dose (1 μM).

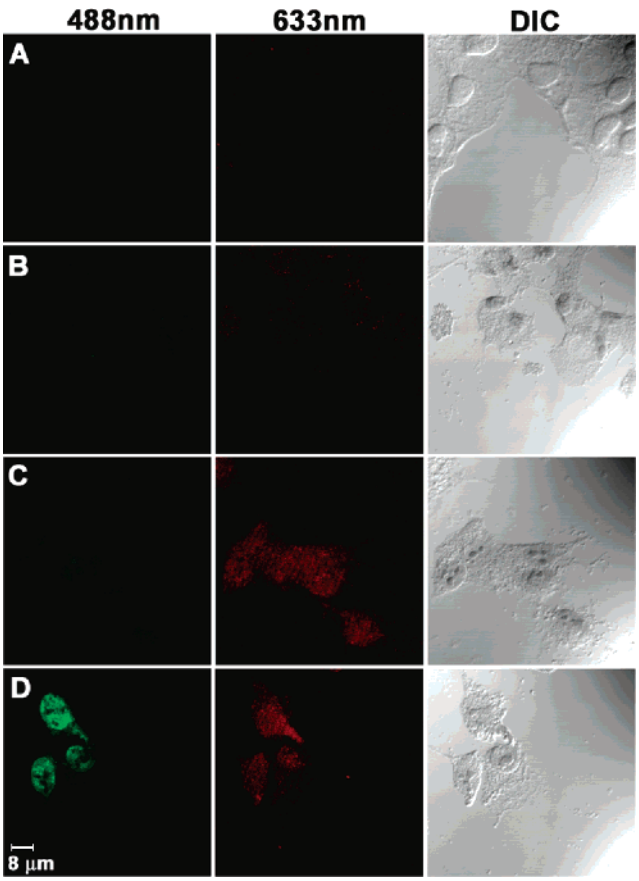

Figure 4. Detection of PDT-induced apoptosis in $HepG_2$ cells by both PDT-BIAS prototype Pyro-GDEVDGSGK-(BHQ-3) (PPB, 200 μM) and an Apoptag assay using confocal microscopy. From left to right: fluorescent image at 488 nm (Fluorescein), 633 nm (Pyro), and DIC image. (A) Cells alone. (B) Cells incubated with PPB, kept in dark and stained with Apoptag show minimal fluorescence increase in both channels ruling out the dark toxicity of PPB. (C) Cells incubated with PPB and treated with 5 J/cm^2 but not stained with Apoptag show increased Pyro fluorescence resulting from PDT-dependent cleavage that does not extensively leak into the 488 nm (Apoptag) channel. (D) In cells incubated with PPB, treated with 5 J/cm^2. and then stained with Apoptag, both Fluorescein and Pyro fluorescence coexist. This confirms that it is the apoptosis causing the PDT-BIAS cleavage.

Discussion. PDT-BIAS is a dual function molecule able to assess its own therapeutic outcome by imaging the extent of apoptosis in situ after PDT treatment. The therapeutic component of PDT-BIAS is pyropheophorbide *a* (a photosensitizer) that has been shown[26] to trigger apoptosis by light-dependent production of singlet oxygen that disrupts the mitochondrial membrane. The critical imaging component is a caspase-3 cleavable sequence since active caspase-3, a crucial executioner protease involved in the progression of controlled cell death, is indicative of apoptosis induction and is frequently used as a

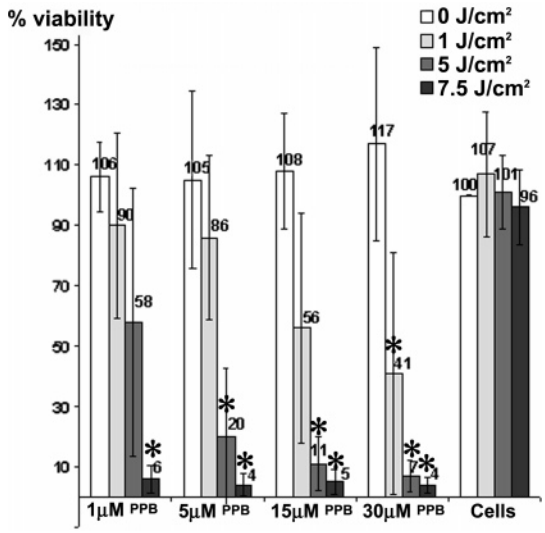

Figure 5. PDT efficacy of Pyro-GDEVDGSGK-(BHQ-3) (PPB) determined by cell viability (MTT) assay. Viability of $HepG_2$ cells after treatment with PPB at four different concentrations (1, 5, 15, and 30 μM) and with three different PDT light doses (1, 5, 7.5 J/cm^2) compared with cells alone that serve as the 100% viable reference. PPB has minimal dark toxicity even for the highest concentration (30 μM, 0 J/cm^2) and good PDT efficacy (1 μM, 7.5 J/cm^2). Comparisons were made to corresponding cell controls by ANOVA (*P < 0.05).

target enzyme for apoptosis imaging.[32] We have shown that PDT-BIAS enters the cytoplasm where it triggers apoptotic events after light treatment. As a consequence, the caspase-3 specific sequence which connects the fluorescent photosensitizer with the quencher in PDT-BIAS is cleaved in vitro after light sensitization. The significant increase of the photosensitizer's fluorescence detected in the light-treated area upon caspase-3 specific cleavage is indicative of PDT-triggered apoptosis.

In our study, PDT-BIAS was cleaved in solution by purified caspase-3 enzyme, and the PDT-induced cleavage was also observed in vitro (cancer cells) by confocal microscopy and flow cytometry. To further demonstrate apoptosis involvement in this cleavage we have used an Apoptag assay and fluorescently labeled antibody to visualize apoptosis-specific DNA cleavage and activated caspase-3, respectively, in PDT-BIAS-treated cancer cells. We observed the coexistence of increased signals from both the cleavage of PDT-BIAS and Apoptag assay/anticaspase-3 labeling for cells treated with drug and PDT compared to those cells treated only with drug. We monitored apoptosis using both PDT-BIAS and commercially available apoptosis sensors and can therefore assert that our PDT-BIAS can be used, unlike most current commercial sensors, as a tool for monitoring PDT-triggered apoptosis in situ. We have also made the first attempt to image PDT-triggered apoptosis in vivo, using an intratumor drug injection (Supporting Information, Figure 6).

Prototype and Targeted PDT-BIAS. In this proof-of-principle study, we introduced a prototype PDT-BIAS comprised of multiple functional modules featuring a photosensitizer for PDT (Pyro), an apoptosis sensing peptide sequence (caspase-3 specific substrate), an apoptosis reporter (fluorescence of photosensitizer generated upon caspase-3 activation), and a quencher to reduce the background fluorescence thus enhancing the sensitivity. All of these components can be exchanged or modified and their properties fine-tuned, for example, by attaching a delivery vehicle for more discriminate in vivo delivery.

Apoptosis Detection. Distinguishing apoptosis from necrosis after PDT treatment is a useful evaluation of new PDT drugs and can be used for optimization of treatment approaches (for example, altering the drug and light dose according to different cancer types). PDT-BIAS can also be used as a membrane-permeant NIR apoptosis sensor for in situ evaluation of other cell-death-causing drugs. Since caspase-3 is exclusively part of the apoptotic machinery, this may be achieved by combining information gained from caspase-3 sensitive probes such as our PDT-BIAS with monitoring the overall cell death marked by Annexin V which is already used as an in situ reporter of cell death, but cannot distinguish apoptosis[5] and necrosis.[33]

Therapy and Detection. PDT-BIAS combines therapy with detection. In order for this study to progress from its preliminary phase, we need to circumvent a few problems such as (1) the low cancer-specificity of our nontargeted probe for better in vivo discrimination, (2) the partial singlet oxygen quenching by the BHQ-3 resulting in slightly lower PDT efficacy, and (3) the light-dependent photobleaching of the photosensitizer's fluorescence (although this photobleaching is minimized by the relatively low light doses required for PDT-induced apoptosis). These problems can be solved by attaching a cancer-specific homing molecule and changing the core components of the PDT-BIAS scaffold to adjust its properties. In conclusion, we have shown that membrane-permeable PDT-BIAS can effectively trigger and image apoptosis upon light exposure in situ.

Experimental Section

The HPLC was run on a Waters 600 controller with a 2996 photodiode array detector and 2475 multi λ fluorescence detector that is used for the analytical HPLC. The eluents are as follows: A = 0.1 M TEAA (pH 7), B = acetonitrile. The method used for all injections is as follows: 90% of A and 10% of B to 100% of B in 45 min, flow: 1.5 mL/min (used for purification) or 1 mL/min (for analysis) on column Zorbax 300SB-C18. The coupling reagents 1-hydroxybenzotriazole (HOBt) and *O*-(benzotriazol-1-yl)-*N*,*N*,*N*′,*N*′-tetramethyluronium hexafluorophosphate (HBTU) were purchased from ACROS and Fluka, respectively. MALDI-ToF was obtained from an Applied Biosystems Voyager DE mass spectrometer, and fluorescence was measured on Perkin-Elmer LS50B luminescence spectrometer. We acquired confocal images using a Leica TCS SP2 confocal microscope. The flow cytometry was run on BD LSRII machine for Pyro (exc. 633 nm, em. 695/40) and Alexa Fluor (exc. 488 nm, em. 530/30) at the Flow Cytometry Resource Laboratory, Abramson Cancer Center, at UPENN. Human hepatoblastoma G_2 ($HepG_2$) cells were obtained from van Berkel's laboratory from University of Leiden in The Netherlands, and KB cells (human epidermoid carcinoma cells) were purchased from ATCC. We used the following buffers for $HepG_2$ cells: complete DMEM (87% DMEM—Dulbecco's modified eagle medium, 10% fetal bovine serum, 1% of 200 mM L-glutamine, 1% of 10000 U pen-strep, 1% of 1 M HEPES) and DMEM containing 0.8% BSA (97% DMEM, 8 g/L of bovine serum albumine, 1% of 200 mM L-glutamine, 1% of 10000 U pen-strep, 1% of 1 M HEPES). The buffers used for KB cells were the following: complete MEM (85% MEM—minimum essential medium, 10% fetal bovine serum, 2% of 1.5 g/L sodium bicarbonate, 1% of 200 mM L-glutamine, 1% of 0.1 mM nonessential amino acids and 1% of 1 mM sodium pyruvate) and MEM containing 0.8% BSA (MEM supplemented with 8 g/L of bovine serum albumine). The Apoptag assay (ApopTag plus Fluorescein in situ apoptosis detection kit S7111) was purchased from Chemicon International. The cleaved caspase-3 antibody (Alexa Fluor 488 Conjugate) for flow cytometry was purchased from Cell Signaling Technology. All compounds prepared for in vitro experiments were first dissolved in DMSO (no more than 1% of total volume) then diluted with 0.1% Tween-80 in DNA—water, filtered through a 0.22

μm filter, and further diluted with an appropriate buffer. The laser for PDT treatment was tuned to 670 nm with fluence rate of 20 mW/cm^2.

PPB Synthesis. For synthesis of immobilized peptide (**1**) see Supporting Information.

Pyro-GD(Boc)E(Boc)VD(Boc)GS(Boc)GK(Mtt)-Sieber Resin (2). After the last Fmoc group cleavage, the resin was washed and Pyro-acid was coupled to the α-NH_2 group of N-terminal Gly. The molar ratio of Pyro/HOBt/HBTU to the peptide on resin was 3:1, the coupling time was 17 h, and the reaction was done in the shake flask in dry NMP. The resin was washed afterward by NMP, capped by 0.3 M acetylimidazol in NMP for 15 min, and washed again by excess of NMP, DCM, and dry methanol. The mixture was transferred from the shake flask and dried under high vacuum.

Pyro-GDEVDGSGK(ϵ-NH_2) (3). Compound **2** was cleaved from resin (33 mg, 8.5 μmol) and deprotected in one step by 50% TFA/5% TIS/DCM for 2 h to yield Pyro-GDEVDGSGK (**3**, PP) with the ϵ-NH_2 group of C-terminal Lys exposed. The compound was precipitated from the cleavage solution by dry ether and prepurified by a few cycles of ether precipitation−DMSO dissolving. Compound **3** (9.6 mg, 7 μmol) was dried under high vacuum and, without further purification, used in the next reaction. Just a small sample was purified by HPLC and the structure confirmed by MALDI-ToF (mass calculated: 1377.64, found: 1377.95).

Pyro-GDEVDGSGK(ϵ-BHQ-3) (4). Crude Pyro-GDEVDGSGK (**3**) (6.8 mg, 4.9 μmol) was dissolved in 50 μL of dry 0.5% DIPEA/DMSO and reacted for 2 h with BHQ-3-NHS (4 mg, 5.1 μmol, purchased from Biosearch Technologies, dissolved in 50 μL of dry DMSO) to give Pyro-GDEVDGSGK-(BHQ-3) (**4**, PPB). The reaction was quenched by precipitation with ether that separates it partially from the redundant BHQ-3-NHS. This final compound was purified by HPLC (the same method as **3**) and dried on speed-vac to obtain 6.5 mg (3.4 μmol) of pure final product **4** that was stored at −20 °C. The purity was checked by analytical HPLC coupled with fluorescence and a UV−vis detector (λ_{max} = 410 nm, $\epsilon \sim 120000$) as well as by MALDI-ToF (mass calculated: 1906.91, found: 1906.21).

Cleavage by Caspase-3 in Solution. The caspase-3 kit (containing the active form of caspase-3 enzyme, caspase-3 inhibitor Ac-DEVD-CHO,[34] and caspase-3 fluorogenic substrate Z-DEVD-AMC) used for fluorescence and HPLC measurements of PPB cleavage was purchased from BD Pharmagen. The buffer used in all measurements contains 20 mM PIPES, 100 mM NaCl, 10 mM DTT, 1 mM EDTA, 0.1% (w/v) CHAPS, 10% sucrose, 0.3% Tween-80, pH 7.2. The molar ratio of caspase-3:PPB-3:inhibitor is 1:200:3000; the incubation time is 3 h. The activity of caspase-3 was checked before every measurement by its ability to cleave the fluorogenic substrate Z-DEVD-AMC. The PPB sample was prepared as a stock solution of 0.25 mM in DMSO and then diluted to the 6.3 μM solution, while 1 mg of inhibitor was diluted by 1 mL of DMSO to generate a 1 mg/mL stock solution. The composition of each sample is as follows: (1) **PPB alone**: 5 μL of PPB stock solution (0.25 mM) was dissolved in 45 μL of DMSO and 150 μL of buffer to yield 6.3 μM PPB solution. (2) **PPB with caspase-3**: 5 μL of PPB stock solution (0.25 mM) was dissolved in 45 μL of DMSO and 150 μL of buffer (6.3 μM PPB solution), and 0.2 μg of caspase-3 was added. (3) **PPB with caspase-3 and inhibitor**: 5 μL of PPB stock solution (0.25 mM) was dissolved in 35 μL of DMSO, then 10 μL of inhibitor (10 μg) was added and diluted with 150 μL of buffer (to yield 6.3 μM PPB and 100 μM inhibitor solution) and finally 0.2 μg of caspase-3 was added. All three solutions were incubated for 3 h at 37 °C, and fluorescence was measured using an excitation wavelength of 410 nm and emission at 674 nm after diluting the samples 60-fold by DMSO. After 50 min, 40 μL of each solution was injected into the HPLC.

Accumulation and Cleavage of PPB in $HepG_2$ Cells. $HepG_2$ cells were grown in 4-well Lab-Tek chamber slides (Naperville, IL) at a density of 50000 cells/well and grown for 24 h in complete DMEM, then rinsed with HBSS (Hank's balanced salt solution) and incubated with 200 μM of the drug in 300 μL of DMEM containing 0.8% BSA at 37 °C for 24 h (except Figure 3E, which is incubated for 30 min). Cells were repeatedly rinsed with HBSS after the incubation, and 300 μL of complete DMEM was added. PDT-treated cells were illuminated by a laser tuned to 670 nm with a 5 J/cm^2 light dose and a 20 mW/cm^2 fluence rate. All cells were fixed 1 hr after PDT by 1% formaldehyde in PBS for 20 min prior to scanning or staining with the Apoptag assay which was performed in accordance with the Chemicon Inl. protocol.

Settings for Confocal Microscopy. Detector slits used: 640−800 nm for detection of Pyro and 497−580 nm for Fluorescein (of Apoptag), with zoom = 2, expander = 3, and resolution 1024 × 1024. The settings (objective; power, gain, and offset for each wavelength respectively) for Figure 3: 40 × objective, 633 nm: 81%, 861.4, −19.7. For Figure 4: 100 × objective, 488 nm: 100%, 757.3, 5; 633 nm: 100%, 753.2, −21.9.

Flow Cytometry Experiment. KB cells (1×10^6) were seeded in T25 flasks and grown for 1 day in complete MEM. The cells were incubated for 12 h with 15 μM PPB in MEM containing 0.8% BSA (1.5 mL/flask), and at the end of incubation the medium was aspirated and cells washed 3 times with 3 mL of PBS and complete MEM was added. Cells intended for PDT were immediately treated with 10 J/cm^2. The cells were carefully harvested 20 h after PDT or drug aspiration by repeated washing first with PBS (most of the PDT-treated cells were already floating) and later with 0.01% Trypsine-EDTA or 0.5 mM EDTA. The cells were fixed with 2% methanol-free formaldehyde in PBS and stained with cleaved caspase-3 antibody (Alexa Fluor 488 conjugate) according to Cell Signaling Technology protocol. Flow cytometry detected FSC/SSC parameters, Pyro (633 nm laser) (cleaved PPB), and Alexa Fluor (488 nm laser) (Antibody staining).

Cell Viability Assay (MTT Assay). $HepG_2$ cells were seeded in clear 96-well plates at a density of 50000 cells/well in 250 μL of complete DMEM and grown overnight at 37 °C. Cells were subsequently rinsed with HBSS and incubated with no or 1, 5, 15, or 30 μM drug in DMEM containing 0.8% BSA (12 wells/concentration) for 20 h. Cells were then rinsed with HBSS, 100 μL of complete DMEM was added, and the cells were treated with three different light doses (by 670 nm laser with 20 mW/cm^2 fluence rate): 3 wells/concentration/light dose with 3 wells/light dose for "light only control" and 3 wells/concentration kept in dark as "drug only control". After incubation for 24 h at 37 °C, the cells were incubated for 2 h with a 0.5 mg/mL solution of MTT in complete DMEM, which was disposed afterward and replaced with 100 μL of 70% 2-propanol in 0.1 M HCl. Absorbance at 570 nm was measured. Data shown in Figure 5 were based on 3−8 different experiments, and the results were expressed as mean ± standard error. Analysis of variance (ANOVA) with Tukey's multiple comparison post hoc testing was used for evaluation of differences between groups. Differences with P value less than 0.05 will be deemed significant.

Acknowledgment. We thank Ponzy Lu and Brian C. Wilson for helpful discussions and André E. X. Brown and Cara Bertozzi for critical comments and suggestions on the manuscript. We also thank William F. DeGrado for access to the MALDI-ToF. This work was supported by the DOD Breast Cancer Research Program DAMD17-03-1-0373 and the NIH Grant U54 CA105008.

Supporting Information Available: Figure 1 showing purity, UV−vis, and MALDI-ToF of PP (**3**); Figure 2 showing purity, UV−vis, and MALDI-ToF of PPB (**4**); Figure 3 showing HPLC of scrambled sequence Pyro-GPLGLARK-(BHQ-3) (sPPB) incubated with caspase-3 for 180 min; Figure 4 showing accumulation of PPB (**4**) inside KB cells monitored by fluorescence microscopy; Figure 5 showing $HepG_2$ cells incubated with scrambled sequence Pyro-GHSSK(BHQ-3)LQL and Pyro-GDEVDGSGK-(BHQ-3) (**4**) and activated by light monitored by confocal microscopy; ANOVA test for MTT study; Figure 6 showing preliminary in vivo experiment; synthesis of Fmoc-GD(Boc)E(Boc)VD(Boc)GS(Boc)-

GK(Mtt)-Sieber (**1**). This material is available free of charge via the Internet at http://pubs.acs.org.

References

(1) Thompson, C. B. Apoptosis in the pathogenesis and treatment of disease. *Science* **1995**, *267*, 1456−1462.
(2) Kaufmann, S. H.; Gores, G. J. Apoptosis in cancer: cause and cure. *Bioessays* **2000**, *22*, 1007−1017.
(3) Van Cruchten, S.; Van Den Broeck, W. Morphological and biochemical aspects of apoptosis, oncosis and necrosis. *Anat., Histol., Embryol.* **2002**, *31*, 214−223.
(4) Vermes, I.; Haanen, C.; Reutelingsperger, C. Flow cytometry of apoptotic cell death. *J. Immunol. Methods* **2000**, *243*, 167−190.
(5) Petrovsky, A.; Schellenberger, E.; Josephson, L.; Weissleder, R.; Bogdanov, A., Jr. Near-infrared fluorescent imaging of tumor apoptosis. *Cancer Res.* **2003**, *63*, 1936−1942.
(6) Bohm, I.; Schild, H. Apoptosis: the complex scenario for a silent cell death. *Mol. Imaging Biol.* **2003**, *5*, 2−14.
(7) Walsh, G. M.; Dewson, G.; Wardlaw, A. J.; Levi-Schaffer, F.; Moqbel, R. A comparative study of different methods for the assessment of apoptosis and necrosis in human eosinophils. *J. Immunol. Methods* **1998**, *217*, 153−163.
(8) Gujral, J. S.; Knight, T. R.; Farhood, A.; Bajt, M. L.; Jaeschke, H. Mode of cell death after acetaminophen overdose in mice: apoptosis or oncotic necrosis? *Toxicol. Sci.* **2002**, *67*, 322−328.
(9) Thornberry, N. A.; Lazebnik, Y. Caspases: enemies within. *Science* **1998**, *281*, 1312−1316.
(10) Dougherty, T. J.; Kaufman, J. E.; Goldfarb, A.; Weishaupt, K. R.; Boyle, D.; et al. Photoradiation therapy for the treatment of malignant tumors. *Cancer Res.* **1978**, *38*, 2628−2635.
(11) Dougherty, T. J.; Gomer, C. J.; Henderson, B. W.; Jori, G.; Kessel, D. et al. Photodynamic therapy. *J. Natl. Cancer I* **1998**, *90*, 889−905.
(12) Rosenkranz, A. A.; Jans, D. A.; Sobolev, A. S. Targeted intracellular delivery of photosensitizers to enhance photodynamic efficiency. *Immunol. Cell Biol.* **2000**, *78*, 452−464.
(13) Wilson, B. C.; Patterson, M. S. The physics of photodynamic therapy. *Phys. Med. Biol.* **1986**, *31*, 327−360.
(14) Niedre, M.; Patterson, M. S.; Wilson, B. C. Direct near-infrared luminescence detection of singlet oxygen generated by photodynamic therapy in cells in vitro and tissues in vivo. *Photochem. Photobiol.* **2002**, *75*, 382−391.
(15) Oleinick, N. L.; Evans, H. H. The photobiology of photodynamic therapy: cellular targets and mechanisms. *Radiat. Res.* **1998**, *150*, S146−S156.
(16) Moor, A. C. Signaling pathways in cell death and survival after photodynamic therapy. *J. Photochem. Photobiol., B* **2000**, *57*, 1−13.
(17) Oleinick, N. L.; Morris, R. L.; Belichenko, I. The role of apoptosis in response to photodynamic therapy: what, where, why, and how. *Photochem. Photobiol. Sci.* **2002**, *1*, 1−21.
(18) Almeida, R. D.; Manadas, B. J.; Carvalho, A. P.; Duarte, C. B. Intracellular signaling mechanisms in photodynamic therapy. *Biochim. Biophys. Acta* **2004**, *2*, 59−86.
(19) Lavie, G.; Kaplinsky, C.; Toren, A.; Aizman, I.; Meruelo, D.; et al. A photodynamic pathway to apoptosis and necrosis induced by dimethyl tetrahydroxyhelianthrone and hypericin in leukaemic cells: possible relevance to photodynamic therapy. *Br. J. Cancer* **1999**, *79*, 423−432.
(20) Kessel, D.; Luo, Y.; Deng, Y.; Chang, C. K. The role of subcellular localization in initiation of apoptosis by photodynamic therapy. *Photochem. Photobiol.* **1997**, *65*, 422−426.
(21) Kessel, D.; Luo, Y. Photodynamic therapy: a mitochondrial inducer of apoptosis. *Cell Death Differ.* **1999**, *6*, 28−35.
(22) Kessel, D. Relocalization of cationic porphyrins during photodynamic therapy. *Photochem. Photobiol. Sci.* **2002**, *1*, 837−840.
(23) Morris, R. L.; Azizuddin, K.; Lam, M.; Berlin, J.; Nieminen, A. L.; et al. Fluorescence resonance energy transfer reveals a binding site of a photosensitizer for photodynamic therapy. *Cancer Res.* **2003**, *63*, 5194−5197.
(24) Porter, A. G.; Janicke, R. U. Emerging roles of caspase-3 in apoptosis. *Cell Death Differ.* **1999**, *6*, 99−104.
(25) MacDonald, I. J.; Morgan, J.; Bellnier, D. A.; Paszkiewicz, G. M.; Whitaker, J. E. et al. Subcellular localization patterns and their relationship to photodynamic activity of pyropheophorbide-a derivatives. *Photochem. Photobiol.* **1999**, *70*, 789−797.
(26) Sun, X.; Leung, W. N. Photodynamic therapy with pyropheophorbide-a methyl ester in human lung carcinoma cancer cell: efficacy, localization and apoptosis. *Photochem. Photobiol.* **2002**, *75*, 644−651.
(27) Zhang, M.; Zhang, Z.; Blessington, D.; Li, H.; Busch, T. M.; et al. Pyropheophorbide 2-deoxyglucosamide: a new photosensitizer targeting glucose transporters. *Bioconjugate Chem.* **2003**, *14*, 709−714.
(28) Chiu, S. M.; Oleinick, N. L. Dissociation of mitochondrial depolarization from cytochrome *c* release during apoptosis induced by photodynamic therapy. *Br. J. Cancer* **2001**, *84*, 1099−1106.
(29) Bellnier, D. A.; Greco, W. R.; Loewen, G. M.; Nava, H.; Oseroff, A. R.; et al. Population pharmacokinetics of the photodynamic therapy agent 2-[1-hexyloxyethyl]-2-devinyl pyropheophorbide-a in cancer patients. *Cancer Res.* **2003**, *63*, 1806−1813.
(30) Chen, J.; Stefflova, K.; Niedre, M. J.; Wilson, B. C.; Chance, B.; et al. Protease-triggered photosensitizing beacon based on singlet oxygen quenching and activation. *J. Am. Chem. Soc.* **2004**, *126*, 11450−11451.
(31) Pham, W.; Weissleder, R.; Tung, C. H. An azulene dimer as a near-infrared quencher. *Angew. Chem., Int. Ed. Engl.* **2002**, *41*, 3659−3662.
(32) Bullok, K.; Piwnica-Worms, D. Synthesis and characterization of a small, membrane-permeant, caspase-activatable far-red fluorescent peptide for imaging apoptosis. *J. Med. Chem.* **2005**, *48*, 5404−5407.
(33) Appelt, U.; Sheriff, A.; Gaipl, U. S.; Kalden, J. R.; Voll, R. E.; et al. Viable, apoptotic and necrotic monocytes expose phosphatidylserine: cooperative binding of the ligand Annexin V to dying but not viable cells and implications for PS-dependent clearance. *Cell Death Differ.* **2005**, *12*, 194−196.
(34) Garcia-Calvo, M.; Peterson, E. P.; Leiting, B.; Ruel, R.; Nicholson, D. W.; et al. Inhibition of human caspases by peptide-based and macromolecular inhibitors. *J. Biol. Chem.* **1998**, *273*, 32608−32613.

JM060146U